The Unusually Slow Unfolding Rate Causes the High Stability of Pyrrolidone Carboxyl Peptidase from a Hyperthermophile, *Pyrococcus furiosus*: Equilibrium and Kinetic Studies of Guanidine Hydrochloride-Induced Unfolding and Refolding†

Kyoko Ogasahara,‡ Mamoru Nakamura,‡ Satomi Nakura,§ Susumu Tsunasawa,§ Ikunoshin Kato,§ Tadashi Yoshimoto,|| and Katsuhide Yutani*,‡

Institute for Protein Research, Osaka University, Suita, Osaka 565-0871, Japan, Biotechnology Research Laboratories, Takara Shuzo Co., Ltd., Sunaike, Nojicho, Kusatsu, Shiga 525-0055, Japan, and School of Pharmaceutical Science, Nagasaki University, Bunkyo-machi, Nagasaki 852-8131, Japan

Received June 18, 1998; Revised Manuscript Received September 8, 1998

ABSTRACT: To elucidate the energetic features of the anomalously high-level stabilization of a hyperthermophile pyrrolidone carboxyl peptidase (*Pf*PCP) from a hyperthermophilic archaeon, *Pyrococcus furiosus*, equilibrium and kinetic studies of the guanidine hydrochloride (GuHCl)-induced unfolding and refolding were carried out with CD measurements at 220 nm in comparison with those from the mesophile homologue (*Ba*PCP) from *Bacillus amyloliquefaciens*. The mutant protein of *Pf*PCP substituted with Ser at both Cys142 and Cys188 (*Pf*C142/188S) was used. The GuHCl unfolding for *Pf*C142/188S and *Ba*PCP was reversible. It was difficult to obtain the equilibrated unfolding curve of the hyperthermophile proteins at temperatures below 50 °C and pH 7, because of the remarkably slow rate of the unfolding. The unfolding for *Pf*C142/188S attained equilibrium after 7 days at 60 °C, resulting in the coincidence between the unfolding and refolding curves. The Gibbs energy change of unfolding, ΔG^{H_2O} (56.6 kJ/mol), for *Pf*C142/188S at 60 °C and pH 7 was dramatically higher than that (7.6 kJ/mol) for *Ba*PCP at 40 °C and pH 7. The unfolding and refolding kinetics for *Pf*C142/188S and *Ba*PCP at both 25 and 60 °C at pH 7 were approximated as a single exponential. The rate constant in water ($k_u^{H_2O}$) of the unfolding reaction for *Pf*C142/188S (1.6×10^{-15} s^{-1}) at 25 °C and pH 7 was drastically reduced by 7 orders of magnitude compared to that (1.5×10^{-8} s^{-1}) for *Ba*PCP, whereas the refolding rates ($k_r^{H_2O}$) in water for *Pf*C142/188S (9.3×10^{-2} s^{-1}) and *Ba*PCP (3.6×10^{-1} s^{-1}) at 25 °C and pH 7 were similar. These results indicate that the greater stability of the hyperthermophile PCP was characterized by the drastically slow unfolding rate.

Proteins from hyperthermophiles maximally express biological functions under extreme conditions near 100 °C, in which the organisms optimally grow (*1*−*5*). Denaturation temperatures of hyperthermophile proteins monitored by differential scanning calorimetry (DSC) are unusually high, near the boiling point of water or higher (*5*−*16*). The molecular origin governing the extraordinary resistance toward heating is potentially significant for understanding the mechanism of stabilization of protein and protein folding and also for developing biotechnological applications. The stability of proteins would basically originate from the combination of many different kinds of forces involved in unique three-dimensional structures. Crystal structures of several hyperthermophile proteins have been determined, and their structural features have been discussed (*17*−*25*). However, the structural features that are responsible for the extra stability or whether there is a common origin of the characteristic of anomalous stability is not known.

For solving the mechanism stabilizing hyperthermophile proteins, the stability in solution should be quantitatively determined, and further, the energetic aspects stabilizing the proteins from a thermodynamic point of view should be elucidated. The thermodynamic stability of a protein is quantitatively defined by the Gibbs energy change upon denaturation ($\Delta G = -RT \ln K$) deduced from the equilibrium constant (K). When postulated as a simple reversible two-state transition, the equilibrium constant ($K = k_u/k_r$) is characterized by the rate constants of unfolding (k_u) and refolding (k_r). The stability thus involves both equilibrium and kinetic aspects. The kinetic study provides important insight together with the equilibrium study for elucidating the thermodynamic and energetic properties stabilizing hyperthermophile proteins. In most of the reported hyperthermophile proteins, however, the stability has been represented as the half-life of activity of proteins incubated at elevated temperatures or in the presence of a denaturant [see the review by Jaenicke et al. (*5*)]. Until now, there have been only a few studies in which the equilibrium and kinetic

† This work was supported in part by a Grant-in-Aid (07280103) for Scientific Research from the Ministry of Education, Science and Culture of Japan to K.Y.

* To whom all correspondence should be addressed: Institute for Protein Research, Osaka University, Yamadaoka, Suita, Osaka 565-0871, Japan. Telephone: 81-6-879-8615. Fax: 81-6-879-8616. E-mail: yutani@protein.osaka-u.ac.jp.

‡ Osaka University.

§ Takara Shuzo Co., Ltd.

|| Nagasaki University.

10.1021/bi9814585 CCC: $15.00
Published on Web 11/21/1998

stabilities of hyperthermophile proteins have been quantitatively evaluated (*11*, *13*, *14*).

In previous studies, we have found that the denaturation temperatures of methionine aminopeptidase (*15*) from a hyperthermophilic archaeon, *Pyrococcus furiosus*, decrease with reducing heating rates in DSC. This suggests that the stability of the hyperthermophile proteins is under kinetic control. In this study, we focused on the kinetic aspect together with the equilibrium stability that characterizes the stability of pyrrolidone carboxyl peptidase (EC 3.4.19.3) (*Pf*PCP)[1] from *P. furiosus*, in comparison with that of the mesophile counterpart (*Ba*PCP) from *Bacillus amyloliquefaciens*.

Pyrrolidone carboxyl peptidase (PCP) specifically removes the L-pyroglutamic acid at the amino terminus of proteins (*26*, *27*). The gene encoding *Pf*PCP has been cloned into *Escherichia coli*, and *Pf*PCP can be expressed in *E. coli*. The subunit of *Pf*PCP consists of 208 amino acid residues with two free Cys residues at positions 142 and 188 (molecular weight of 22 800) (*16*). *Ba*PCP has 215 amino acid residues (molecular weight of 23 400) (*28*). Cys188 in *Pf*PCP is partly oxidized in the native state (N. N. Khechinashvili et al., in preparation). To exclude the complexity in unfolding and refolding reactions due to the oxidation of SH groups, a mutant protein (*Pf*C142/188S) substituted with Ser at both Cys142 and Cys188 was then used. In this study, guanidine hydrochloride (GuHCl)-induced unfolding and refolding of *Pf*PCP and *Pf*C142/188S were examined from both equilibrium and kinetic points of view in comparison with the mesophile counterpart. The anomalous high stability of the hyperthermophile PCP was revealed to originate from the unusually slow rate of the unfolding reaction. We will address the energetic base stabilizing *Pf*PCP.

MATERIALS AND METHODS

Bacterial Strains and Protein Expression. The wild type PCP (*Pf*PCP) from *P. furiosus* and its mutant protein (*Pf*C142/188S) substituted with Ser at both Cys142 and Cys188 were expressed in *E. coli* strain JM109/pPCP3 and *E. coli* strain JM109/pPCP3022, respectively (*16*).

Bacterial Cultures and Purification of PCPs. The production of *Pf*PCP and *Pf*C142/188S proteins was induced by addition of isopropyl β-thiogalactopyranoside at a concentration of 1 mM per liter of the culture medium when the absorbance at 660 nm of the medium reached about 0.6. After induction, the culture was continued for about 20 h at 37 °C while it was shaken. *Pf*PCP and *Pf*C142/188S were purified as described previously (*16*). Purified PCP (*Ba*PCP) from *B. amyloliquefaciens* was obtained as described previously (*28*). Purified PCPs gave a single band on SDS−PAGE.

Guanidine hydrochloride (GuHCl) (specially prepared reagent grade) from Nacalai Tesque (Kyoto, Japan) was used without further purification. Other chemicals were reagent grade.

The protein concentrations were estimated from the absorbance at 278.5 nm, using an $E^{1\%}$ of 6.6 for *Pf*PCP and *Pf*C142/188S and 8.3 for *Ba*PCP using a cell with a light path length of 10 mm. These values were determined on the basis of a protein assay by the Lowry method with bovine serum albumin as a protein standard.

CD Spectra. Far- and near-UV CD spectra were recorded on a Jasco J-720 spectropolarimeter equipped with an NEC personal computer. Far- and near-UV CD spectra were scanned 16 and 36 times, respectively, at a scan rate of 20 nm/min, using a time constant of 0.25 s. The light path length of the cell used was 0.118 mm in the far-UV region and 10 mm in the near-UV region. The protein concentrations were 0.8−2.3 mg/mL. For calculation of the mean residue ellipticity, [θ], the mean residue weights were assumed to be 109.3 for *Pf*PCP and *Pf*C142/188S and 108.8 for *Ba*PCP.

Equilibrium Experiments on Guanidine Hydrochloride-Induced Unfolding and Refolding. For unfolding, *Pf*PCP, *Pf*C142/188S, and *Ba*PCP were incubated in GuHCl at various concentrations and at different temperatures for various times. For refolding, the protein which completely unfolded in the presence of GuHCl at high concentrations was diluted with 20 mM buffer with 2 mM EDTA and 0.1 mM dithioerythritol (DTE) containing various concentrations of GuHCl, and the diluted protein solution was incubated at the desired temperature until the refolding reached equilibrium. The unfolding and refolding were monitored by measuring the CD at 220 nm and 25 °C after incubation for the desired times at different temperatures. CD measurements were carried out with a Jasco J-500 recording spectropolarimeter equipped with a data processor (model DP-501). The fraction of unfolding (f_u) was calculated from eq 1

$$f_u = (b_n^0 + a_n[C] - y)/(b_n^0 + a_n[C] - b_u^0 - a_u[C]) \quad (1)$$

where f_u is the fraction of the unfolded state, y the CD value at a given concentration of GuHCl, and [C] the concentration of GuHCl. b_n^0 and b_u^0 are the CD values for the native and the unfolded states at 0 M GuHCl, respectively. a_n and a_u are the slopes of the pre- and post-transition baselines, respectively. GuHCl unfolding data were analyzed by the linear extrapolation model (*29*, *30*) assuming a two-state transition, according to the following equations.

$$N \Leftrightarrow U \quad (2)$$

$$K = f_u/(1 - f_u) \quad (3)$$

$$\Delta G = -RT \ln K \quad (4)$$

$$\Delta G = \Delta G^{H_2O} + m[C] \quad (5)$$

$$f_u = \exp^{-(\Delta G^{H2O} + m[C])/RT}/[1 + \exp^{-(\Delta G^{H2O} + m[C])/RT}] \quad (6)$$

where K and ΔG are the equilibrium constant of the unfolding reaction and the Gibbs energy change upon unfolding, respectively. m is the slope of the linear correlation between ΔG and the GuHCl concentration [C]. ΔG^{H_2O} is the Gibbs energy change upon unfolding in the absence of GuHCl (in water). f_u in eq 6 is represented as a function of the concentration of GuHCl. We used a computer program to produce a least-squares fit of the experimental data in GuHCl unfolding curves to eq 6 to obtain ΔG^{H_2O}.

Kinetic Experiments on Unfolding and Refolding. The reactions of unfolding and refolding were followed by CD at 220 nm. The CD measurements were carried out with a Jasco J-720 recording spectropolarimeter equipped with an

[1] Abbreviations: PCP, pyrrolidone carboxyl peptidase; *Pf*PCP, wild type PCP from *P. furiosus*; *Pf*C142/188S, mutant PCP from *P. furiosus* substituted with Ser at Cys142 and Cye188; *Ba*PCP, PCP from *B. amyloliquefaciens*; DTE, dithioerythritol.

NEC personal computer. The unfolding reactions of the proteins were initiated by GuHCl concentration jumps to various concentrations. The refolding reactions of the proteins were induced by dilution of the GuHCl concentration of the protein solution, in which the proteins were completely unfolded in the presence of GuHCl at high concentrations. For preparing the completely unfolded proteins, *Pf*C142/188S was incubated in 7.0 M GuHCl at pH 7 and 60 °C for 1 day, and *Ba*PCP in 5.0 M GuHCl at pH 7 and 25 °C for 1 day. In the cases of both unfolding and refolding, 1 volume of the native or unfolded protein was rapidly added manually to 10 volumes of GuHCl solution at various concentrations in the cell with a 10 mm light path length while the mixture was being stirred using a spinning mixer with a magnetic stirrer, and CD at 220 nm was recorded as a function of time. The dead time of this procedure was 1 s (*31*, *32*).

The kinetic data were analyzed with software (*33*) for curve fitting by a nonlinear least-squares method using the equation

$$A(t) - A(\infty) = \sum A_i e^{-k_i t} \qquad (7)$$

where $A(t)$ is the value of CD at a given time t, $A(\infty)$ is the value when no further change is observed, which is related to the equilibrium value expected from the corresponding equilibrium transition curve, k_i is the apparent rate constant of the ith kinetic phase, and A_i is the amplitude of the ith phase.

All the equilibrium and kinetic experiments were performed in 20 mM Tris-HCl buffer (pH 7) containing 2 mM EDTA and 0.1 mM DTE. The protein concentrations when CD measurements were taken were 0.007−0.02 mg/mL. CD at 220 nm was measured in a cell with a 10 mm light path length with a thermostatically controlled cell holder.

RESULTS

CD Spectra of PCPs. Figure 1 displays the far- and near-UV CD spectra of *Pf*PCP, *Pf*C142/188S, and *Ba*PCP at pH 7.0 and 25 °C. In the far-UV CD spectra, the negative CD values around 220 nm for *Pf*C142/188S were slightly larger than those for *Pf*PCP (curves 1 and 2 in Figure 1a), although the near-UV CD spectrum of *Pf*C142/188S was similar to that of *Pf*PCP (curves 1 and 2 in Figure 1b). This suggests that the substitution slightly affects the content of the secondary structure. The far-UV CD spectra of *Pf*PCP and *Ba*PCP resembled each other, indicating the similarity of the secondary structures of the two PCPs. However, the near-UV CD spectrum of *Pf*PCP significantly differed from that of *Ba*PCP (curves 1 and 3 in Figure 1b). The numbers of Trp and Tyr residues are zero and eight, respectively, in *Pf*PCP and two and five, respectively, in *Ba*PCP. Six Phe residues are involved in both *Pf*PCP and *Ba*PCP. The difference in the near-UV CD spectra of *Pf*PCP and *Ba*PCP probably arises from the difference in the number of aromatic residues. For *Pf*PCP, *Pf*C142/188S, and *Ba*PCP, the far-UV CD spectra at the high concentration of GuHCl (curves 1′−3′ in panel in Figure 1a) were typical shapes characteristic of the unfolded forms of general proteins.

Equilibrium Studies of GuHCl-Induced Unfolding and Refolding. The GuHCl-induced unfolding of PCPs was monitored by CD measurements at 220 nm at various pHs and different temperatures. Figure 2a shows the time-dependent GuHCl unfolding curves of *Pf*PCP at pH 7 and 25 °C. Although the CD values in the presence of GuHCl at >7 M seemed to be constant after 28 days, the negative CD values in the transition region decreased with a prolonged incubation period, resulting in a shift of the transition curves toward lower concentrations of GuHCl and a decrease in the GuHCl concentration at the midpoint. This means that a much longer time is needed for unfolding to attain equilibrium. Pre- and post-transition baselines depended on the GuHCl concentration. The negative CD values of the pretransition baseline decreased with extended incubation time, but the baselines linearly depended on the GuHCl concentration. Hence, the fraction of the unfolding form at each concentration of GuHCl was calculated according to eq 1.

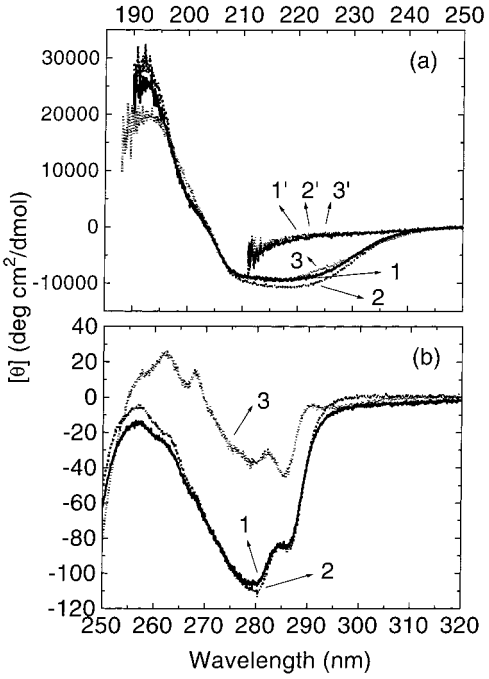

FIGURE 1: CD spectra of *Pf*PCP, *Pf*C142/188S, and *Ba*PCP at pH 7 and 25 °C. Potassium phosphate buffer (20 mM) was used as the buffer solution: (a) far-UV CD spectra and (b) near-UV CD spectra. Curves 1 are the spectra of *Pf*PCP in the native state. Curves 2 are the spectra of *Pf*C142/188S in the native state. Curves 3 are the spectra of *Ba*PCP in the native state. Curves 1′−3′ are the spectra of *Pf*PCP, *Pf*C142/188S, and *Ba*PCP, respectively, in the unfolded state. The CD spectra of the unfolded states were measured at 25 °C, after the protein solutions in 6.0 M GuHCl at pH 7 were incubated for 1 day at 60 °C to promote the unfolding reaction of *Pf*PCP and *Pf*C142/188S. The spectrum of *Ba*PCP in the unfolded state was also measured at 25 °C after incubation for 1 day in 5.0 M GuHCl at 40 °C and pH 7.

To examine whether the GuHCl-induced unfolding of *Pf*PCP is reversible, the refolding curves were examined under various conditions by monitoring the changes in the CD value at 220 nm. The refolding experiments were performed by diluting the GuHCl concentration of the *Pf*PCP solution incubated for 1 day in 7 M GuHCl at 60 °C and pH 7, in which the unfolding of *Pf*PCP attained equilibrium as judged by the lack of further changes in the CD values. The transition curves of the refolding for *Pf*PCP at various temperatures from 25 to 60 °C at pH 7 attained equilibrium after 1 day, but the unfolding curves below 50 °C at pH 7 even after 45 days were inconsistent with the equilibrated refolding curves (data not shown). When the temperature

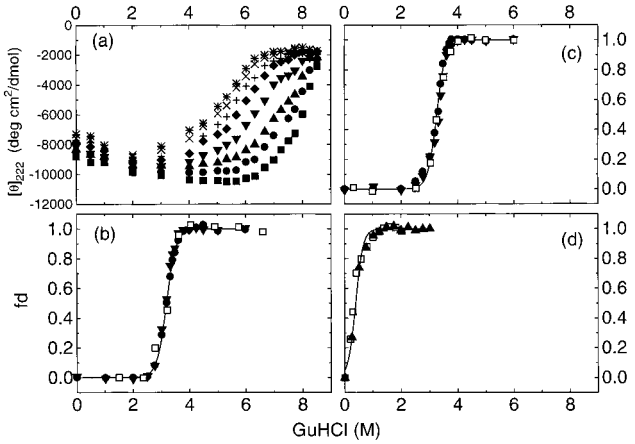

FIGURE 2: GuHCl-induced unfolding and refolding curves of *Pf*PCP, *Pf*C142/188S, and *Ba*PCP at pH 7 and various temperatures. The unfolding and refolding were monitored by the CD values at 220 nm. For the unfolding, the proteins in different concentrations of GuHCl were incubated for various times at constant temperatures. For the refolding, the proteins of the completely unfolded protein solutions in GuHCl at high concentrations and pH 7 were diluted to various concentrations of GuHCl at constant temperature. The buffer solution used was 20 mM Tris-HCl (pH 7) containing 2 mM EDTA and 0.1 mM DTE for *Pf*PCP and *Ba*PCP and the same buffer without EDTA and DTE for *Pf*C142/188S. (a) Time dependence of unfolding curves for *Pf*PCP at 25 °C and pH 7: CD values after incubation for (■) 1 day at 25 °C and after (●) 2, (▲) 3, (▼) 7, (◆) 14, (+) 21, (×) 28, and (∗) 45 days. In panels b−d, the unfolding and refolding curves were normalized according to eq 1. Closed and open symbols represent the data points for unfolding and refolding, respectively. Solid lines are the curves fitted to eq 6. (b) *Pf*PCP at 60 °C and pH 7: unfolding after 7 (●) and 14 days (▼) and refolding after 1 day (□). (c) *Pf*C142/188S at 60 °C and pH 7: unfolding after 7 (●) and 14 days (▼) and refolding after 1 day (□). (d) *Ba*PCP at 40 °C and pH 7: unfolding after 1 day (▲) and refolding after 6 h (□).

was elevated to 60 °C at pH 7, the unfolding curve of *Pf*PCP after 7 days was identical to that after 14 days and also could be overlaid on the refolding curve, as shown by the normalized curves in Figure 2b. This revealed that the unfolding curves of *Pf*PCP at 60 °C and pH 7 could attain equilibrium after 7 days and confirms that the GuHCl-induced unfolding of *Pf*PCP is reversible. The discrepancy between the unfolding and refolding curves at temperatures below 50 °C was found to be caused by the fact that the unfolding did not yet reach equilibrium.

In the case of *Pf*C142/188S, the unfolding transition curves after 1 day at 25 °C at pH 7 did not coincide with the refolding curve (data not shown), although the refolding curves equilibrated after 1 day. At 60 °C and pH 7, the unfolding curve after 7 days was coincident with those after 14 days and also the refolding curve after 1 day (Figure 2c). Thus, it was found that the GuHCl-induced unfolding for *Pf*C142/188S was reversible and could attain equilibrium after 7 days at 60 °C and pH 7.

For *Ba*PCP, the unfolding after 7 days at 25 °C and pH 7 was inconsistent with the refolding curve (data not shown). At 40 °C and pH 7, the unfolding curve attained equilibrium after 1 day (Figure 2d). At 60 °C and pH 7, the complete transition curves of the unfolding and refolding with a pretransition baseline could not be obtained, because *Ba*PCP was partly unfolded at this temperature even in the absence of GuHCl (data not shown).

Table 1: Thermodynamic Parameters of Equilibrium GuHCl Unfolding for *Pf*PCP, *Pf*C142/188S, and *Ba*PCP at pH 7[a]

protein	temperature (°C)	C_m (M)	m for ΔG^{H_2O} (kJ mol^{-1} M^{-1})	ΔG^{H_2O} (kJ/mol)	K^{H_2O}
*Pf*PCP	60	3.2	-17.3 ± 0.5	54.4 ± 1.7	2.8×10^{-9}
*Pf*C142/188S	60	3.4	-17.4 ± 1.3	56.6 ± 4.1	1.3×10^{-9}
*Ba*PCP	40	0.4	-19.5 ± 1.8	7.6 ± 0.8	5.4×10^{-2}

[a] Unfolding experiments were performed under the conditions described in the legend of Figure 2b−d. C_m is the GuHCl concentration of the midpoint in the transition. m is the slope of the GuHCl concentration dependence of ΔG. The values of ΔG^{H_2O} and m were estimated by fitting the data points to eq 6. The data points in the unfolding curves after 14 days were used for *Pf*PCP and *Pf*C142/188S at 60 °C and after 1 day for *Ba*PCP at 40 °C.

The reversible unfolding curves for three kinds of PCPs, which were consistent with each refolding curve, were highly cooperative. When a two-state transition for the unfolding of all of the PCPs is assumed, as described in eq 2, the thermodynamic parameters for the unfolding were estimated according to eqs 3−6, as listed in Table 1. The GuHCl concentration (3.4 M) at the midpoint of the transition of *Pf*C142/188S at 60 °C was remarkably higher than that (0.4 M) of *Ba*PCP at 40 °C.

Kinetic Studies of GuHCl-Induced Unfolding and Refolding. The equilibrium study highlighted the fact that the unfolding rate of the hyperthermophile protein was extremely slow, in particular, under moderate conditions (at 25 °C and pH 7). However, the unfolding curve of *Pf*C142/188S attained equilibrium after 7 days at 60 °C and pH 7 (Figure 2c). The kinetics of the GuHCl-induced unfolding and refolding for *Pf*C142/188S and *Ba*PCP were then examined at both temperatures of 25 and 60 °C at pH 7. The unfolding reaction was initiated by concentration jumps to various concentrations of GuHCl. Before the refolding experiments were started, *Pf*C142/188S was incubated in 7.0 M GuHCl at 60 °C and pH 7 for 1 day and *Ba*PCP in 5.0 M GuHCl at 25 °C and pH 7 for 1 day so they would be completely unfolded. The refolding reaction was induced by dilution of the GuHCl concentration of the sample. Typical kinetic curves for the unfolding and refolding at pH 7 and 25 °C, as followed by the change in CD values at 220 nm, are shown in Figure 3.

Unfolding progressions of *Pf*C142/188S and *Ba*PCP at both 25 and 60 °C and pH 7 could be approximated by a single exponential in eq 7 at various final concentrations of GuHCl (Figure 3a). The detectable changes in the CD value at various concentrations of GuHCl at 60 °C for *Pf*C142/188S were equivalent to the CD value as expected from the equilibrium unfolding transition in Figure 2c. The relative amplitudes of *Pf*C142/188S at 25 °C and *Ba*PCP at 25 and 60 °C according to eq 7 were also estimated to be 100%.

For the refolding reactions for *Pf*C142/188S and *Ba*PCP, a large amount of the CD value at 220 nm was rapidly recovered within the dead time (1 s). After that, the negative CD values at 220 nm increased toward the equilibrium values at a given concentration of GuHCl. In all cases, the progress curves could be approximated by a single exponential and the relative amplitudes for detectable phases maximally accounted for 55% (Figure 3b). These results indicate that the refolding of *Pf*C142/188S and *Ba*PCP occur via at least two steps, suggesting the presence of the undetectable early

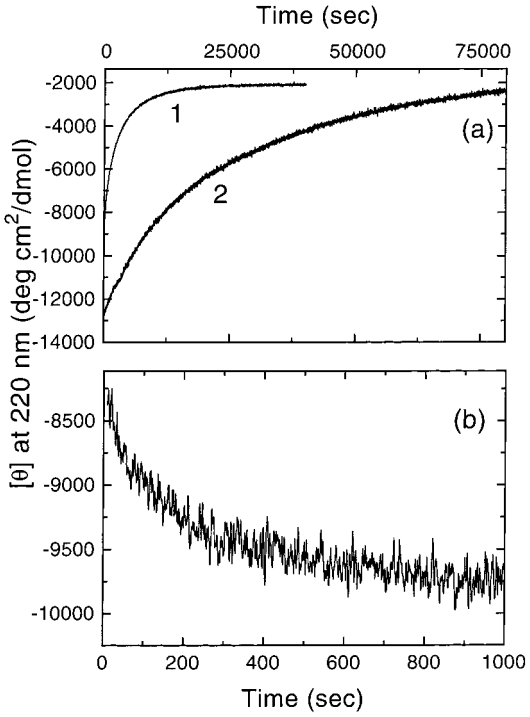

FIGURE 3: Typical kinetic progress curves of unfolding and refolding of *Pf*C142/188S and *Ba*PCP at pH 7 and 25 °C. The reaction progress was followed by the change in CD at 220 nm. The unfolding (a) and refolding (b) were induced by concentration jumps of GuHCl: (a) curve 1, [GuHCl] jump from 0 to 3.92 M for *Ba*PCP; and curve 2, [GuHCl] jump from 0 to 7.72 M for *Pf*C142/188S; and (b) [GuHCl] jump from 7 to 0.80 M for *Pf*C142/188S.

folding intermediates in the folding process. The refolding reaction of *Ba*PCP at 60 °C and pH 7 was not precisely analyzed, because *Ba*PCP was partly unfolded at this temperature.

Dependences of Apparent Rate Constants of Unfolding and Refolding Reactions on the GuHCl Concentration. Figure 4 displays the GuHCl concentration dependence of the logarithms of the apparent rate constants (k_{app}) of the unfolding and refolding for *Pf*C142/188S in comparison with those for *Ba*PCP at 25 and 60 °C, respectively, and pH 7. In the unfolding and refolding for *Pf*C142/188S and *Ba*PCP, the log k_{app} linearly correlated with the GuHCl concentration. The k_{app} values of the unfolding for *Pf*C142/188S and *Ba*PCP could not be compared in the same concentration range of GuHCl, since the unfolding zone of *Pf*C142/188S shifted toward high concentrations of GuHCl relative to that of *Ba*PCP. On the contrary, the refoldings of *Pf*C142/188S and *Ba*PCP at 25 °C were able to be measured in the same concentration region of GuHCl.

The rate constant for unfolding, k_u, is generally found to increase with increasing GuHCl concentration [C] according to eq 8

$$\log k_u = \log k_u^{H_2O} + m_2[C] \quad (8)$$

where $k_u^{H_2O}$ is the rate constant in water (in the absence of GuHCl) (*34*). In the unfolding zone, k_{app} ($=k_u + k_r$) should be close to k_u because $k_u \gg k_r$, where k_r is the rate constant for refolding. In the cases of both *Pf*C142/188S and *Ba*PCP, the respective unfolding and refolding reactions could be measured only in the unfolding and refolding zones. Thus, the $k_u^{H_2O}$ value was estimated by linear extrapolation to 0 M GuHCl using eq 8. The rate constant of refolding ($k_r^{H_2O}$) in water was also estimated by linear extrapolation to 0 M GuHCl. The kinetic parameters are presented in Table 2. It was noticeable that the value of $k_u^{H_2O}$ of *Pf*C142/188S was drastically lower than that of *Ba*PCP by a factor of 10^7 at 25 °C and 10^6 at 60 °C. On the contrary, the rate of refolding in water ($k_r^{H_2O}$) of *Pf*C142/188S at 25 °C was similar to that of *Ba*PCP.

The value of the rate constant can be converted to the activation Gibbs energy change ($\Delta G^{\ddagger}$) according to transition state theory (*35*). The activation Gibbs energy changes in water ($\Delta G^{\ddagger H_2O}$) to the transition state from the native and unfolded states can be calculated from $k_u^{H_2O}$ and $k_r^{H_2O}$, respectively, by the Eyring equation (eq 9)

$$\Delta G^{\ddagger H_2O} = RT \ln(k_B T/hk^{H_2O}) \quad (9)$$

where k_B and h are Boltzmann's and Planck's constants, respectively. The results are listed in Table 2.

DISCUSSION

Reversibility of Chemical Unfolding. An attempt to thermodynamically characterize the stability of hyperthermophile proteins had been plagued by the irreversibility of its heat denaturation (*6*−*9*, *11*, *14*, *15*, *36*). Recently, two kinds of small DNA binding proteins with molecular weights of 7K, Sac7d (*12*) and Sso7d (*13*), have been reported to be reversibly heat-denatured. The present *Pf*PCP and its Cys mutant protein are reversibly heat-denatured (N. N. Khechinashvili et al., in preparation). On the other hand, the GuHCl-induced unfolding of glyceraldehyde-3-phosphate dehydrogenase from *Thermotoga maritima* has been shown to be reversible (*37*), although the heat denaturation of the protein is irreversible (*6*, *36*). The chemical unfolding of Sac7d is also reversible (*12*). The reversible unfolding−refolding system is advantageous not only for analyzing qualitatively the stability of a protein but also for elucidating the folding mechanism. PCP from *P. furiosus* has tractable characteristics with respect to the reversibility of unfolding; although a very long time was needed for equilibrating, GuHCl-induced unfolding (Figure 2) was completely reversible as well as the heat denaturation near pH 3 (N. N. Khechinashvili et al., in preparation). We could then examine the energetic features of the unfolding and refolding of *Pf*C142/188S.

High Equilibrium Stability of the Hyperthermophile PCP. The equilibrium stability (ΔG^{H_2O}) of a protein in water can be obtained from equilibrium and kinetic experiments, if unfolding is a two-state transition. In equilibrium experiments, GuHCl unfolding curves of *Pf*PCP, *Pf*C142/188S, and *Ba*PCP were well fitted to a two-state transition expressed by eq 6 (Figure 2). The thermodynamic parameters obtained from the equilibrated unfolding curves of *Pf*PCP and *Pf*C142/188S at 60 °C and *Ba*PCP at 40 °C are listed in Table 1. In a kinetic experiment based on a two-state transition (eq 2), on the other hand, the equilibrium constant of unfolding in water, K^{H_2O}(kin), can be obtained from $k_u^{H_2O}/k_r^{H_2O}$, yielding ΔG^{H_2O}(kin) (Table 2). For *Pf*C142/188S at 60 °C and pH 7, the ΔG^{H_2O} values, 56.6 and 57.8 kJ/mol, obtained from equilibrium and kinetic methods, respectively, coincided with each other, indicating that the assumption of a two-state transition is appropriate. The equilibrium stability of the

Table 2: Kinetic Parameters of Unfolding and Refolding in Water at pH 7 for *Pf*C142/188S and *Ba*PCP

protein	temperature (°C)	log $k_u^{H_2O}$ (s^{-1})	$k_u^{H_2O}$ [a] (s^{-1})	$\Delta G_u^{\ddagger H_2O}$ (kJ/mol)	log $k_r^{H_2O}$ (s^{-1})	$k_r^{H_2O}$ [a] (s^{-1})	$\Delta G_r^{\ddagger H_2O}$ (kJ/mol)	K^{H_2O}(kin) [b]	ΔG^{H_2O}(kin) [c] (kJ/mol)
*Pf*C142/188S	25	-14.8 ± 0.4	1.6×10^{-15}	157.5	-1.0 ± 0.2	9.3×10^{-2}	78.9	1.7×10^{-14}	78.6
*Ba*PCP	25	-7.8 ± 0.2	1.5×10^{-8}	117.7	-0.4 ± 0.1	3.6×10^{-1}	75.9	4.2×10^{-8}	41.8
*Pf*C142/188S	60	-8.5 ± 0.2	3.4×10^{-9}	135.9	0.6 ± 0.1	3.8	78.2	8.9×10^{-10}	57.8
*Ba*PCP	60	-2.6 ± 0.1	2.7×10^{-3}	98.3	nd [d]	nd [d]	nd [d]	nd [d]	nd [d]

[a] $k_u^{H_2O}$ and $k_r^{H_2O}$ were estimated from extrapolation to zero GuHCl on the straight line in Figure 4. [b] If the unfolding−refolding reaction of PCPs in water is a two-state transition, the equilibrium constant, K^{H_2O}(kin), in water can be calculated from $k_u^{H_2O}/k_r^{H_2O}$. [c] The Gibbs energy change in water, ΔG^{H_2O}(kin), was calculated from the rate constants of unfolding and refolding reactions. [d] nd means the refolding reaction of *Ba*PCP could not be measured, because *Ba*PCP was partly unfolded at 60 °C in the absence of GuHCl.

hyperthermophile PCP could not be compared with that of the mesophile counterpart at the same temperature (Table 1), because the GuHCl-induced unfolding of the hyperthermophile PCP did not attain equilibrium at the temperature in which the unfolding of the mesophile PCP is usually examined (<40 °C). The kinetic experiments could give the ΔG^{H_2O} values at the same temperature (25 °C) for *Pf*C142/188S and *Ba*PCP with the assumption of a two-state transition. The ΔG^{H_2O}(kin) value (78.6 kJ/mol) of *Pf*C142/188S at 25 °C and pH 7 was indeed strongly high compared to that (41.8 kJ/mol) of *Ba*PCP (Table 2).

Unusually Slow Rate of the Unfolding Reaction of the Hyperthermophile PCP. The unfolding rate ($k_u^{H_2O}$) of *Pf*C142/188S in water at 25 °C and pH 7 was 1.6×10^{-15} s^{-1} (Table 2). When simply translated, this value corresponds to a relaxation time of 20 million years. This means that *Pf*C142/188S does not unfold on a biologically relevant time scale under physiological conditions of mesophiles. The fact that the GuHCl-induced unfolding curves of *Pf*PCP and *Pf*C142/188S could not reach equilibrium (Figure 2) under moderate conditions resulted from their unusually slow rate of unfolding. The $k_u^{H_2O}$ value (1.5×10^{-8} s^{-1}) of *Ba*PCP at 25 °C and pH 7 was also lower than those of general globular proteins; for example, the $k_u^{H_2O}$ value is on the order of 10^{-4} s^{-1} under similar conditions in the case of the tryptophan synthase α subunit (*31*, *32*). This decrease in the $k_u^{H_2O}$ value of *Ba*PCP may be due to a tetrameric structure which involves much more interaction necessary for maintenance of the native form. The unfolding rates were increased on the order of 10^6 and 10^5-fold for *Pf*C142/188S and *Ba*PCP, respectively, by increasing the temperature from 25 to 60 °C (Table 2). Compared with the unfolding rate of *Ba*PCP, the unfolding rate of *Pf*C142/188S was drastically slow; the $k_u^{H_2O}$ value decreased 10^7-fold at 25 °C and 10^6-fold at 60 °C (Table 2).

On the other hand, the refolding rate ($k_r^{H_2O}$) in water for *Pf*C142/188S at 25 °C and pH 7 was similar in order to that of *Ba*PCP and corresponded to values for general globular proteins from mesophiles. The difference (10^{-7} s^{-1}) in the unfolding rates between the hyperthermophile PCP and the mesophile counterpart at 25 °C largely surpassed the difference in the refolding rates (Table 2). These results indicate that the unfolding rate is the crucial factor determining the stability of *Pf*C142/188S. These findings evidently reveal that the origin of the extra equilibrium stability of the hyperthermophile PCP in the moderate-temperature region arises from the drastically slow unfolding rate.

It has been reported that rubredoxin from *P. furiosus* unfolds much more slowly than its mesophile counterpart; the heat denaturation rate at 100 °C of hyperthermophile rubredoxin at pH 7 is lower by 10^3 orders of magnitude than that of the mesophile counterpart (*38*). It has been conceivable that the very slow unfolding rate at neutral pH of the hyperthermophile rubredoxin may result from a mild surface "clamping" effect exerted by the salt bridges (*38*). In the case of D-glyceraldehyde-3-phosphate dehydrogenase from *T. maritima*, 96 h is needed to obtain the GuHCl unfolding curve at 25 and 58 °C at pH 7 (*39*). The rate constant of heat denaturation at 100 °C and pH 6.6 of the D-glyceraldehyde-3-phosphate dehydrogenase has been calculated to be 0.027 min^{-1}. Disruption of the ionic network by mutation leads to enhancement of the unfolding rate of this protein, suggesting the importance of ion pairs for a decrease in the unfolding rate (*36*). In the present *Pf*PCP, the molecular origin of the reduction of the unfolding rate cannot be explained by the amino acid sequence alignment between *Pf*PCP and *Ba*PCP. We are attempting to determine the origin on the basis of the crystal structure of *Pf*PCP (T. Tsukihara et al., in preparation).

Energy Diagram of the Native, Transition, Intermediate, and Unfolded States. The energy defining the stability of a protein correlates with changes in Gibbs energies between the states existing in the unfolding−refolding process. The states, in general, are the native, unfolded, intermediate(s), and transition states. To estimate the stability of a protein and elucidate the stabilization mechanism, it is important to determine the absolute value of Gibbs energy for each state, but the absolute values are not obtained experimentally. However, the difference in the energies between the two states can be experimentally measured by the equilibrium and kinetic studies.

The kinetic experiments on *Pf*C142/188S and *Ba*PCP suggested the existence of an intermediate state (I) in the early stage of the folding process, because the amplitudes observed in the refolding kinetics for all the PCPs were below 55%. This means that the process from the U to I states is too rapid to observe and that the energy barrier between them is not high. The limiting state ($T^{\ddagger}$) in the folding process should be in the process from the I to N states. In the case of *Pf*C142/188S at 60 °C and pH 7, the ΔG^{H_2O}(kin) (57.8 kJ/mol) obtained from the kinetic method was nearly identical with the ΔG^{H_2O} (56.6 kJ/mol) from the equilibrium method (Tables 1 and 2). That is, the difference (57.8 kJ/mol) between $\Delta G_u^{\ddagger H_2O}$ and $\Delta G_r^{\ddagger H_2O}$ is equivalent to the ΔG^{H_2O} value from the equilibrium method. This implies that the energy level of the I state for *Pf*C142/188S at 60 °C and pH 7 is comparable to that of the U state and that there is no stable intermediate in the process from the D to N states for *Pf*C142/188S. According to these values, the energy diagram of *Pf*C142/188S at 60 °C and pH 7 is illustrated in

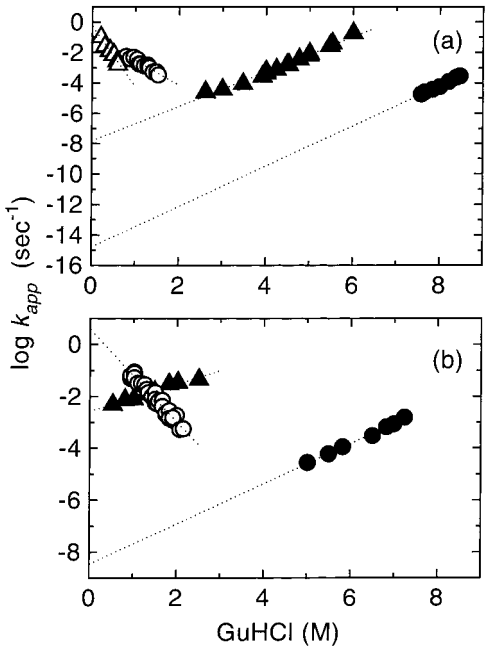

FIGURE 4: GuHCl concentration dependence of the apparent rate constants (k_{app}) of the unfolding and refolding kinetics of *Pf*C142/188S and *Ba*PCP at 25 and 60 °C and pH 7. Panels a and b depict the data at 25 and 60 °C, respectively. The closed and open symbols depict the data points of the unfolding and refolding, respectively, reactions: (● and ○) *Pf*C142/188S and (▲ and △) *Ba*PCP. The dotted lines represent the lines obtained from a least-squares method for log k_{app}.

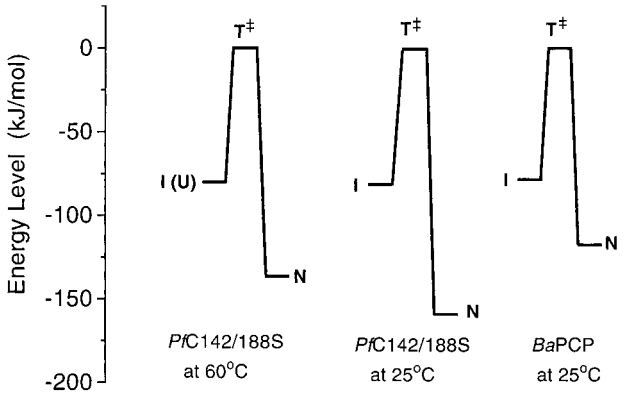

FIGURE 5: Energy coordinate diagrams between the native (N), transition (T‡), intermediate (I), and unfolded (U) states in the folding process in water for *Pf*C142/188S and *Ba*PCP. The diagrams are illustrated using the energy levels of the T‡ states as a reference. For energy levels between the states, the values [ΔG^{H_2O}(kin), $\Delta G_u^{\ddagger H_2O}$, and $\Delta G_r^{\ddagger H_2O}$] obtained from the kinetic method (Table 2) were used. The energy levels of the U and I states for *Pf*C142/188S at 60 °C and pH 7 were assumed to be identical as noted in the text.

Figure 5. The existence of an undetectable early folding intermediate (I) for many mesophile proteins has been reported and assumed to be a molten globule state (*31*, *40*, *41*). The process of unfolding and refolding for *Pf*C142/188S might also be observed to be more complicated under different conditions (N. N. Khechinashvili et al., in preparation). The detailed experiments on the refolding process for *Pf*PCP will be reported in the future.

For *Pf*C142/188S and *Ba*PCP at 25 °C and pH 7, ΔG^{H_2O} could not be obtained from equilibrium methods. Figure 5 shows the energy diagrams of *Pf*C142/188S and *Ba*PCP at 25 °C and pH 7, using the values obtained from the kinetic experiments (Table 2) and the energy levels of the T‡ state as a reference.

These diagrams express three kinds of energetic features for *Pf*C142/188S. First, the activation Gibbs energy change from N to I states ($\Delta G_u^{\ddagger H_2O}$) for *Pf*C142/188S at 25 °C was higher by 40 kJ/mol than that for *Ba*PCP. This means that the energy barrier in going from the N to T‡ states is very high in *Pf*C142/188S. Second, the activation Gibbs energy change from the I to T‡ states ($\Delta G_r^{\ddagger H_2O}$) does not show a big difference between PCPs from the hyperthermophile and the mesophile. Third, the stability [ΔG^{H_2O}(kin)] of the N state relative to the I state of *Pf*C142/188S was substantially higher than that of the mesophile counterpart. From Figure 5, it is easy for us to understand that the extraordinary stabilization of PCP from *P. furiosus* was characterized by the unusually slow unfolding rate and a very high energy barrier in the direction from the N to T‡ state. Recently, it has been reported that the hyperthermostability of a rubredoxin is accompanied by a higher activation free energy of unfolding from the native state and that there is a direct correlation between the degree of thermostability and the magnitude of the unfolding activation free energy among different rubredoxins (*38*).

REFERENCES

1. Stetter, K. O. (1982) *Nature 300*, 258−260.
2. Stetter, K. O., Fiala, G., Huber, G., Huber, R., and Segerer, G. (1990) *FEMS Microbiol. Rev. 75*, 117−124.
3. Adams, M. W. W. (1990) *FEMS Microbiol. Rev. 75*, 129−238.
4. Adams, M. W. W. (1993) *Annu. Rev. Microbiol. 47*, 627−658.
5. Jaenicke, R., Schurig, H., Beaucamp, N., and Ostendorp, R. (1996) *Adv. Protein Chem. 48*, 181−269.
6. Wrba, A., Schweiger, A., Schultes, V., Jaenicke, R., and Zavodszky, P. (1990) *Biochemistry 29*, 7584−7592.
7. Klump, H., Ruggiero, J. D., Kessel, M., Park, J.-B., Adams, M. W. W., and Robb, F. T. (1992) *J. Biol. Chem. 267*, 22681−22685.
8. Laderman, K. A., Davis, B. R., Krutzsch, H. C., Lewis, M. S., Griko, Y. V., Privalov, P. L., and Anfinsen, C. B. (1993) *J. Biol. Chem. 268*, 24394−24401.
9. Klump, H. H., Adams, M. W. W., and Robb, F. T. (1994) *Pure Appl. Chem. 66*, 485−489.
10. McAfee, J. G., Edomondson, S. P., Datta, P. K., Shriver, J. W., and Gupta, R. (1995) *Biochemistry 34*, 10063−10077.
11. DeDecker, B. S., O'Brien, R., Fleming, P. J., Geiger, J. H., Jackson, S. P., and Sigler, P. B. (1996) *J. Mol. Biol. 264*, 1072−1084.
12. McCrary, B. S., Edomondson, S. P., and Shriver, J. W. (1996) *J. Mol. Biol. 264*, 784−805.
13. Knapp, S., Karshikoff, A., Berndt, K. D., Christova, P., Atanasov, B., and Ladenstein, R. (1996) *J. Mol. Biol. 264*, 1132−1144.
14. Pfeil, W., Gesierich, U., Kleemann, G. R., and Sterner, R. (1997) *J. Mol. Biol. 272*, 591−596.
15. Ogasahara, K., Lapshina, E. A., Sakai, M., Izu, Y., Tsunasawa, S., Kato, I., and Yutani, K. (1998) *Biochemistry 37*, 5939−5946.
16. Tsunasawa, S., Nakura, S., Tanigawa, T., and Kato, I. (1998) *J. Biochem. (Tokyo) 124*, 778−783.
17. Day, M. W., Hsu, B. T., Joshua-Tor, L., Park, J.-B., Zhou, Z. H., Adams, M. W. W., and Rees, D. C. (1992) *Protein Sci. 1*, 1494−1507.
18. Russell, R. J. M., Ferguson, J. M. C., Hough, D. W., Danson, M. J., and Taylor, G. L. (1997) *Biochemistry 36*, 9983−9994.
19. Yip, K. S. P., Stillman, T. J., Britton, K. L., Artymiuk, P. J., Baker, P. J., Sedelnikova, S. E., Engel, P. C., Pasquo, A.,

Chiaraluce, R., Consalvi, V., Scandurra, R., and Rice, D. W. (1995) *Structure 3*, 1147−1158.
20. Korndorfer, I., Steipe, B., Huber, R., Tomschy, A., and Jaenicke, R. (1995) *J. Mol. Biol. 246*, 511−521.
21. Chan, M. K., Mukund, S., Kletzin, A., Adams, M. W. W., and Rees, D. C. (1995) *Science 267*, 1463−1469.
22. Hennig, M., Darimont, B., Sterner, R., Kirschner, K., and Jansonius, J. N. (1995) *Structure 3*, 1295−1305.
23. Lim, J.-H., Yu, Y. G., Han, Y. S., Cho, S.-J., Ahn, B.-Y., Kim, S.-H., and Cho, Y. (1997) *J. Mol. Biol. 270*, 259−274.
24. Knapp, S., DeVos, W. M., Rice, D., and Ladenstein, R. (1997) *J. Mol. Biol. 267*, 916−932.
25. Tahirov, T. H., Oki, H., Tsukihara, T., Ogasahara, K., Yutani, K., Ogata, K., Izu, Y., Tsunasawa, S., and Kato, I. (1998) *J. Mol. Biol. 284*, 101−124.
26. Doolittle, R. F., and Armentrout, R. W. (1968) *Biochemistry 7*, 516−521.
27. Szewczuk, A., and Mulczyk, M. (1969) *Eur. J. Biochem. 8*, 63−67.
28. Yoshimoto, T., Shimoda, T., Kitazono, A., Kabashima, T., Ito, K., and Tsuru, D. (1993) *J. Biochem. (Tokyo) 113*, 67−73.
29. Pace, C. N. (1975) *CRC Crit. Rev. Biochem. 3*, 1−43.
30. Pace, C. N. (1986) *Methods Enzymol. 131*, 266−280.
31. Ogasahara, K., and Yutani, K. (1994) *J. Mol. Biol. 236*, 1227−1240.
32. Ogasahara, K., and Yutani, K. (1997) *Biochemistry 36*, 932−940.
33. Sugawara, T., Kuwajima, K., and Sugai, S. (1991) *Biochemistry 30*, 2698−2706.
34. Kuwajima, K., Mitani, M., and Sugai, S. (1989) *J. Mol. Biol. 206*, 547−561.
35. Eyring, H. (1935) *Chem. Phys. Rev. 17*, 65−77.
36. Pappenberger, G., Schurig, H., and Jaenicke, R. (1997) *J. Mol. Biol. 274*, 676−683.
37. Schultes, V., and Jaenicke, R. (1991) *FEBS Lett. 290*, 235−238.
38. Cavagnero, S., Debe, D. A., Zhou, Z. H., Adams, M. W. W., and Chan, S. I. (1998) *Biochemistry 37*, 3369−3376.
39. Tomschy, A., Bohm, G., and Jaenicke, R. (1994) *Protein Eng. 7*, 1471−1478.
40. Kuwajima, K. (1989) *Proteins: Struct., Funct., Genet. 6*, 87−103.
41. Ptitsyn, O. B. (1992) in *Protein Folding* (Creighton, T. E., Ed.) pp 243−300, W. H. Freeman and Company, New York.

BI9814585